Importance of outer-sphere and aggregation phenomena in the relaxation properties of phosphonated gadolinium complexes with potential applications as MRI contrast agents

Mourad Elhabiri[a], Sabah Abada[b], Mohamadou Sy[b], Aline Nonat[b], Philippe Choquet[c,d,e], David Esteban-Gómez[f], Claudio Cassino[g], Carlos Platas-Iglesias[f], Mauro Botta[g] and Loïc J. Charbonnière[b]

[a] Laboratoire de Chimie Bioorganique et Médicinale, UMR 7509 CNRS-Université de Strasbourg, ECPM, 25 rue Becquerel, 67087 Strasbourg Cedex (France)

[b] Laboratoire d'Ingénierie Moléculaire Appliquée à l'Analyse, IPHC, UMR 7178, CNRS- Université de Strasbourg, ECPM, 25 rue Becquerel, 67087 Strasbourg Cedex (France)

[c] Preclinical Imaging Lab - UF6237, Pôle d'imagerie, Hôpitaux Universitaires de Strasbourg, Strasbourg (France)

[d] Icube, équipe MMB, CNRS, Université de Strasbourg, Strasbourg (France)

[e] Fédération de Médecine Translationnelle de Strasbourg, Faculté de Médecine, Université de Strasbourg, Strasbourg (France)

[f] Departamento de Química Fundamental, Universida de da Coruña, Campus da Zapateira-Rúa da Fraga 10, 15008 A Coruña (Spain)

[g] Dipartimento di Scienze e Innovazione Tecnologica, Università del Piemonte Orientale, Viale T. Michel 11, 15121 Alessandria (Italy)

Abstract

A series composed of a tetra-, a tris- and a bisphosphonated ligand based on a pyridine scaffold (L^4, L^3 and L^2, respectively) was studied within the frame of lanthanide (Ln) coordination. The stability constants of the complexes formed with lanthanide cations (Ln=La, Nd, Eu, Gd, Tb, Er and Lu) were determined by potentiometry in aqueous solutions (25.0 °C, 0.1 M NaClO$_4$), showing that the tetraphosphonated complexes are among the most stable Ln^{III} complexes reported in the literature. The complexation of L^4 was further studied by different titration experiments using mass spectrometry and various spectroscopic techniques including UV/Vis absorption, and steady state and time-resolved luminescence (Ln=Eu and Tb). Titration experiments confirmed the formation of highly stable [LnL^4] complexes. ^{31}P NMR experiments of the LuL^4 complex revealed an intramolecular interconversion process

which was studied at different temperatures and was rationalized by DFT modelling. The relaxivity properties of the Gd^{III} complexes were studied by recording their ^{1}H NMRD profiles at various temperatures, by temperature dependent ^{17}O NMR experiments (Gd**L^4**) and by pH dependent relaxivity measurements at 0.47 T (Gd**L^3** and Gd**L^2**). In addition to the high relaxivity values observed for all complexes, the results showed an important second-sphere contribution to relaxivity and pH dependent variations associated with the formation of aggregates for Gd**L^2** and Gd**L^3**. Finally, intravenous injection of Gd**L^4** to a mouse was followed by dynamic MRI imaging at 1.5 T, which showed that the complex can be immediately found in the blood stream and rapidly eliminated through the liver and in large part through the kidneys.

Keywords: imaging agents; lanthanide; luminescence; phosphonate; relaxivity

Introduction

Magnetic resonance imaging (MRI) has become an inescapable tool in the clinical diagnostic toolbox, providing exquisite images of soft tissues with a large range of contrast. This success is in part due to the large improvements brought by contrast agents, and in particular those based on gadolinium complexes.[1] The more or less close contact of water molecules with the paramagnetic Gd^{III} centers results in an important shortening of the longitudinal (T_1) and transverse (T_2) relaxation times of the proton nuclei of water molecules. Even if numerous contrast agents are currently used in clinical practice, there is still a large number of reports on new Gd^{III} complexes aiming at improving the basic relaxivity properties of the probes or targeting specific applications with the use of "smart" contrast agents.[2] Among those, there is a growing interest in phosphonated complexes,[3] as the introduction of these functions or the replacement of carboxylic acid by phosphonic ones have proved to play a significant role on the relaxivity of Gd^{III} complexes.[4]

First, phosphonic acid possesses two dissociation constants, the second one being generally slightly below neutral pH.[5] Phosphonate functions are found to be twice negatively charged near the biological window, allowing for strong electrostatic interactions with metal cations in general[6] and lanthanide ions in particular.[7] As a second point, it has been noticed that the basicity of the amines of phosphonated analogues of amino acids is increased by the presence of the phosphonate function,[8] with a concomitant increase of the stability of the complexes formed with cations.[5] A third important aspect in the comparison of phosphonate and carboxylate functions is the larger steric hindrance brought by the former. A typical example is the comparison of the Gd^{III} complexes of DOTA (1,4,7,10-tetraazacyclododecane-1,4,7,10-tetrakisacetic acid) and its phosphonated analogue DOTP. While the numerous studies on [Gd(DOTA)] complexes showed its coordination sphere to be completed by the presence of one water molecule,[9] those on [Gd(DOTP)][10] confirmed the absence of this supplementary coordination due to the bulkier substituents. These results are in line with other studies showing that the hydration numbers of Gd^{III} complexes decreased by one unit when more than one carboxylate functions are replaced by phosphonate ones.[11] Finally, phosphonate functions induce large second-sphere interactions with water molecules or cations in solution.[12]

Within the frame of our search for highly efficient complexes for molecular imaging, we have been interested in the design of polyphosphonated chelates for luminescence,[7, 13] or radiochemical applications.[14] In this study, we report on the coordination behavior of a series of bis-, tris- and tetraphosphonated ligands (Scheme 1) with lanthanide cations and we particularly inspect the influence of the number of phosphonic coordinating units on the relaxation properties of the corresponding Gd^{III} chelates.
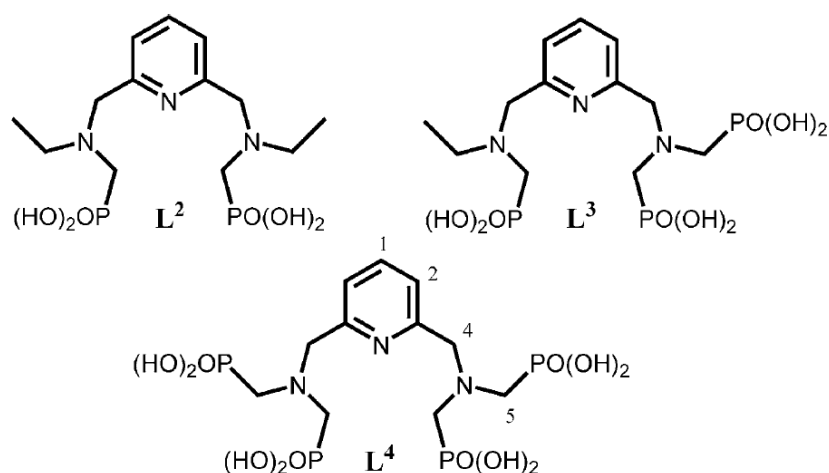
Scheme 1. Molecular structures of ligands $\mathbf{L}^2$ to $\mathbf{L}^4$ with numbering Scheme used for ^{1}H NMR spectral assignment of $\mathbf{L}^4$.

Results and discussion

In order to get insight into the complexation behavior of the ligands with lanthanide cations, we first recorded some titration experiments in which the evolution of the absorption and emission spectra of the ligands were monitored as a function of added cations into the solutions. As an example, the titration of ligand $\mathbf{L}^4$ by Tb[III] is depicted in Figure 1.

From 0 to one equivalent of added Tb, both absorption and emission spectral changes showed monotonous variations attributed to the formation of a first species with a one to one metal to ligand ratio. The fluorescence titration revealed a typical behavior associated with the coordination of Tb[III] to the ligand, that translates into a Tb centered emission upon ligand excitation (λ_{exc}=265 nm), that is, an antenna effect.[15] After one equivalent, the luminescence dropped, pointing to the formation of new species. A striking phenomenon was observed in the absorption titration for Ln/$\mathbf{L}^4$ (Ln=Eu and Tb) molar ratios between 2 and 2.5. The baseline of the spectra gradually drifted, indicating the formation of nano/microparticles that result in light scattering in the cell. The same observation could be made for Eu (Figure S1), with the same drift for ratios between 2 and 2.5.

The composition of the Ln$\mathbf{L}^4$ complexes (Ln=Eu[III] and Tb[III]) was further confirmed in solution by recording the ES/MS spectra of solutions containing equimolar amounts of the cations and ligand in water (Figures S2 and S3). For both complexes, the major species detected corresponded to a [Ln$\mathbf{L}^4$] composition, as evidenced by the isotopic distribution observed for the Eu[III] complex with the presence of [151]Eu and [153]Eu isotopes. The luminescence properties (excited state lifetime and luminescence quantum yield) of equimolar solutions of the ligands with Eu or Tb were determined in water and deuterated water and the results are gathered in Table 1.

It is to be noticed that the reported lifetimes have to be taken as indicative values calculated from mono-exponential fits of the data, despite the evidences that point to the presence of mixtures of complexes with different lifetimes, probably resulting from the complex acid–base equilibria present in solution (see below). It is thus not surprising that the calculated hydration numbers, that is, the number of water molecules directly coordinated to the Ln[III] cations, are rarely integer values. The overall luminescence quantum yields of this family of complexes are modest to poor and always one order of magnitude better for Tb than for Eu, as generally observed for pyridine based lanthanide complexes.[17]
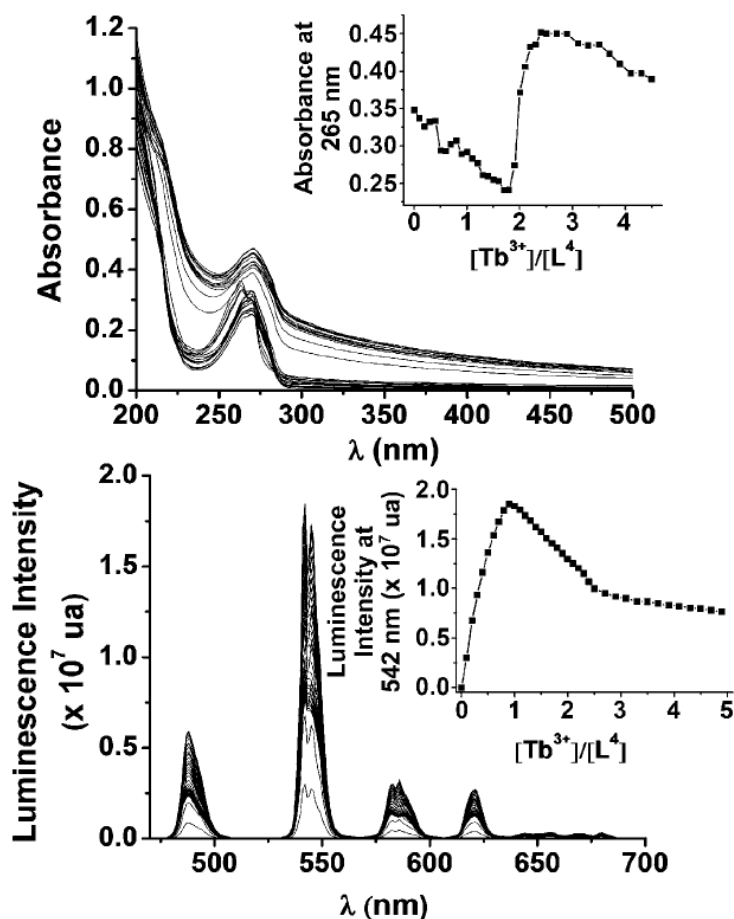
Figure 1. Top: Evolution of the absorption spectra of a solution of L^4 ($c=8.5\times10^{-5}$ M, 0.01 M TRIS/HCl, pH 7.0) upon addition of TbCl$_3$·6H$_2$O (inset: evolution of the absorbance at 265 nm). Bottom: Evolution of the emission spectra of the same solutions (λ_{exc}=265 nm, inset: evolution of the emission intensity at 545 nm).

Table 1. Spectroscopic properties of equimolar mixtures of ligands and Eu or Tb in water and heavy water.

	τ_{H_2O} [ms]	τ_{D_2O} [ms]	ϕ_{H_2O} ($\times$ 100)	$q^{[a]}$
EuL^2	0.364	1.43	0.02	2.2
TbL^2	1.17	2.40	0.36	1.9
EuL^3	0.35	1.07	0.036	2.0
TbL^3	0.93	1.34	0.32	1.3
EuL^4	0.57	2.21	0.12	1.3
TbL^4	1.52	2.90	10.6	1.3

[a] Calculated according to reference [16], estimated error ±15 %.

Considering the prior evidence of the formation of a one to one metal to ligand complex, the thermodynamic stability constants for the formation of lanthanide complexes with ligands L^2 to L^4were determined by potentiometry for equimolar concentrations of lanthanide salts and of the ligands using the values of the

protonation constants previously determined for $\mathbf{L^2}$ to $\mathbf{L^4}$,[18] and taking from the literature the values for the hydrolysis constants of the lanthanide ions.[19]

Table 2 summarizes the newly determined stability constants obtained for $\mathbf{L^2}$ and $\mathbf{L^3}$, together with those previously reported for $\mathbf{L^4}$.[4b] When possible, the protonation constants of the complexes were also determined.

Table 2. Thermodynamic stability constants and protonation constants for the complexes formed with ligands $\mathbf{L^2}$ to $\mathbf{L^4}$ and various Ln^{III} cations along the series and corresponding values of pLn.[a]

	La	Nd	Eu	Gd	Tb	Er	Lu
$\log K_{ML^4}$ [b]	25.5(4)	27.1(3)	25.7(3)	–	29.7(6)	29.7(1)	29.3(4)
$\log K_{ML^4H}$ [b]	9.4(4)	8.8(3)	9.4(3)	–	7.6(7)	7.8(1)	7.4(6)
$\log K_{ML^4H_2}$ [b]	7.3(6)	6.6(4)	7.5(4)	–	[c]	[c]	[c]
$\log K_{ML^3}$	16.3(1)	16.8(1)	–	16.95(9)	–	16.8(1)	[c]
$\log K_{ML^3H}$	8.0(2)	7.9(2)	–	nd	–	nd	[c]
$\log K_{ML^3H_2}$	7.6(2)	7.4(2)	–	nd	–	nd	[c]
$\log \beta_{ML^3H_2}$	15.6(3)	15.3(3)	–	14.6(1)		14.7(2)	
$\log K_{ML^3H_3}$	4.7(2)	4.7(2)	–	4.5(1)	–	4.8(3)	[c]
$\log K_{ML^2}$	10.14(4)	10.66(5)	–	11.22(5)	–	11.15(3)	[c]
$\log K_{ML^2H}$	9.19(5)	9.35(6)	–	9.16(6)	–	9.25(4)	[c]
$\log K_{ML^2H_2}$	7.42(5)	7.40(6)	–	7.21(6)	–	7.90(4)	[c]
pLn$_{L^4}$	20.6	21.3	20.9	–	22.6	22.7	21.9
pLn$_{L^3}$	11.3	11.4	–	10.6	–	10.8	[c]
pLn$_{L^2}$	7.3	8.0	–	8.2	–	8.3	[c]
pLn$_{DOTA}$ [20]	17.8	17.8	18.4	19.6	19.6	19.6	20.3
pLn$_{DOTP}$ [21]	21.5	21.2	21.5	22.5	22.6	24.3	24.3

[a] pLn values are defined by pLn=$-\log[Ln^{III}]_{free}$ at pH 7.0 for [Ln^{III}]=1 μM and [L]=10 μM.[22]
[b] According to reference [4b].
[c] Precipitation of the complexes precludes accurate determination. The hydrolysis constants of the free Ln^{3+}cations have been taken into account in the statistical processing ($\log K_{LaOH}=-8.83$; $\log K_{NdOH}=-8.20$; $\log K_{EuOH}=-7.78$; $\log K_{GdOH}=-7.85$; $\log K_{TbOH}=-7.66$; $\log K_{ErOH}=-7.54$; $\log K_{LuOH}=-7.29$). n.d.=not determined with good accuracy (only the global constant was determined and is given due to the close values of K_{ML^3H} and $K_{ML^3H_2}$.

As anticipated for acyclic chelators, the increase of the binding constants follows a monotonous trend (Figure 2 and Table 2) with the increasing number of phosphonates borne by the ligand. As it was previously noted, the stability of the complexes formed with $\mathbf{L^4}$ is very high, almost as stable as the complexes formed with DOTP. In contrast, the loss of a single phosphonate function resulted in a dramatic decrease of the stability constant (or pLn) values for ligand $\mathbf{L^3}$, the values dropping of more than ten log units (Figure 2). The loss of a second phosphonate function leading to $\mathbf{L^2}$ also resulted in a drop of the stability, but the amplitude of this decrease is far less important (Table 2). Further loss of phosphonate unit would lead to weak chelator (pLn ~6) as exemplified by the stability constants measured for a related system lacking phosphonate moieties (cy$_2$PYAN, $\log K_{LLa}=2.1$ and $\log K_{LGd}=5.6$ and $\log K_{LLu}=6$).[23]
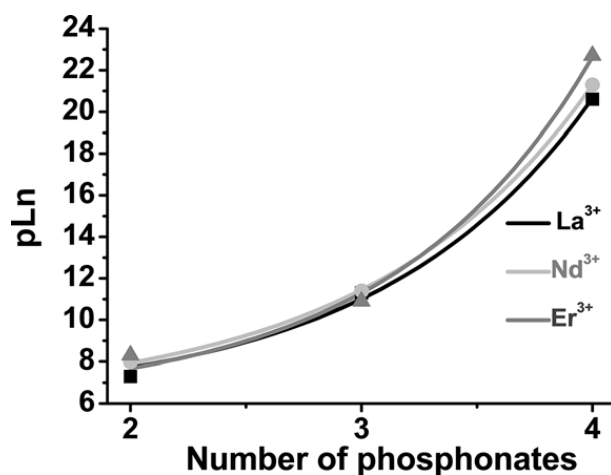
Figure 2. pLn[III] values for La[III] (square), Nd[III] (circle) and Er[III] (triangles) complexes as a function of the number of phosphonates borne by L^2, L^3 and L^4.

Solution structure and dynamics of LnL^4 complexes

The solution ^{1}H, ^{13}C and ^{31}P NMR spectra of the diamagnetic LaL^4 and LuL^4 complexes were recorded in D$_2$O solution at pD 10.9. At this pD, the predominant species in solution is expected to be the fully deprotonated form, as demonstrated by potentiometric measurements (see above). The ^{1}H NMR spectrum of the La[III] complex recorded at 298 K shows only five signals (Figure 3), which suggests an effective C_2v symmetry of the complex in solution. This is confirmed by the ^{13}C spectrum, which consists of five signals for the 11 carbon nuclei of the ligand backbone.
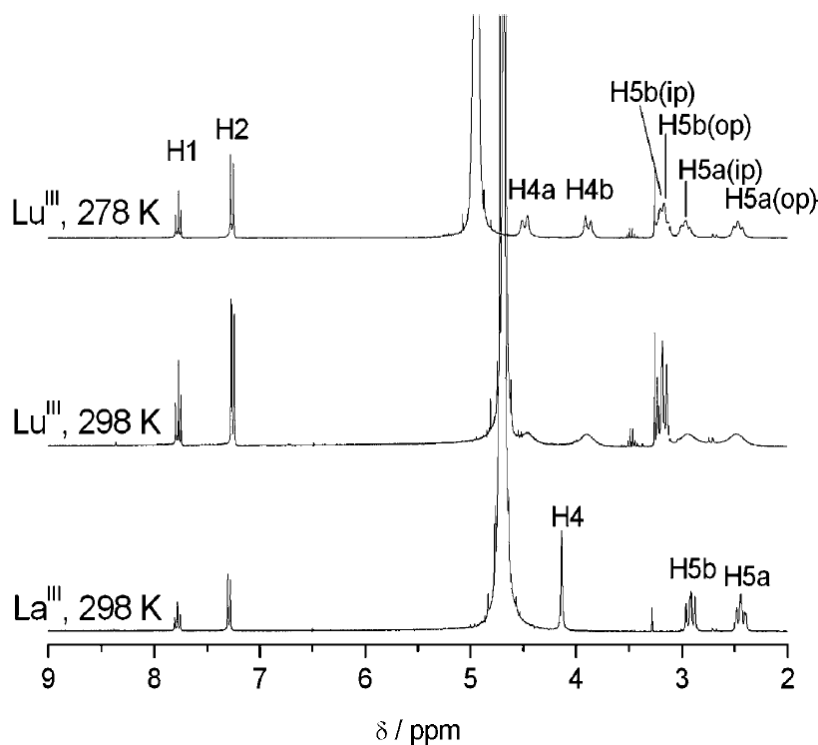

Figure 3. ^{1}H NMR spectra of the La[III] and Lu[III] complexes of L^4 recorded in D$_2$O solution at different temperatures (pD 10.9); see Scheme 1 for H labelling.

The ^{13}C NMR resonance due to the methylenephosphonate groups is split into a doublet of doublets by spin coupling to the adjacent phosphorous ($^1J_{PC}=143.1$ Hz) and to that three bonds away ($^3J_{PC}=8.9$ Hz). Similar coupling constants have been previously observed for Ln[III] complexes with ligands containing methylenephosphonate groups.[24,31] The ^{31}P NMR spectrum shows a single resonance at 19.9 ppm, which confirms an effective C_{2v} symmetry of the complex in solution with the four methylenephosphonate groups of the ligand being equivalent. The assignments of the proton signals are given in Table S1 (Supporting Information). The ^{1}H NMR signal due to H4 is observed as a singlet, while the protons of the methylenephosphonate groups give two multiplets consistent with an ABX spectrum (where X is the ^{31}P nucleus). Thus, the geminal proton nuclei of methylenephosphonate groups are not equivalent.

The proton spectrum of Lu**L**[4] recorded at 298 K (Figure 3) shows broad signals for the methylene groups, indicating the presence of intramolecular dynamic exchange processes in solution. The spectrum recorded at 278 K exhibits a better resolution, as pointed out in our previous communication,[4c] and it is consistent with an effective C_2 symmetry of the complex in solution (Table S1). This is confirmed by the ^{31}P NMR spectrum recorded at 278 K, which shows two signals at 18.9 and 21.6 ppm (Figure 4).

Above this temperature these two signals gradually broaden, and then coalesce at a temperature close to 323 K. Thus, the ^{1}H and ^{31}P NMR spectra of Lu**L**[4] recorded at low temperature show different signals for the in-plane and out-of-plane methylenephosphonate groups with respect to the average plane formed by the pyridine unit and the metal ion (Scheme 2).
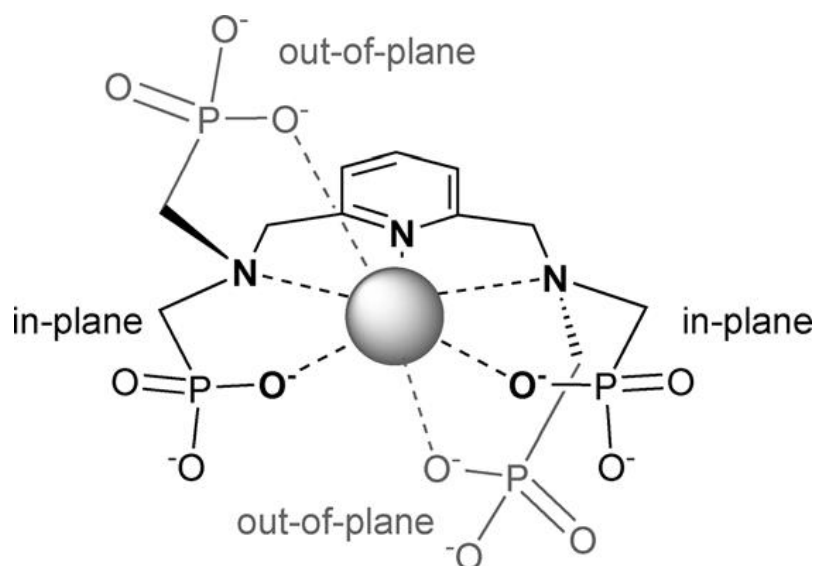
Scheme 2. In-plane (*ip*) and out-of-plane (*op*) methylenephosphonate groups in Ln**L**[4] complexes.

DFT calculations provide ^{31}P NMR chemical shifts of 16.1 and 13.5 ppm for the *ip* and *op* methylenephosphonate groups, respectively. These values compare reasonably well with the experimental ones (21.6 and 18.9 ppm, respectively), particularly taking into account the systematic deviations observed previously for calculated ^{13}C NMR shifts obtained using similar methodologies.[25] Thus, the ^{31}P NMR signal due to *ip* groups is more deshielded than those corresponding to *op* ones, probably as a consequence of the deshielding effect of the pyridine ring current. Once the ^{31}P NMR signals were assigned, a full assignment of the ^{1}H NMR signals was obtained from the cross-peaks observed in the two-dimensional HMBC experiment, which gave strong cross peaks relating the ^{31}P NMR signal at 21.6 ppm to the ^{1}H signal at 2.93 ppm, and the ^{31}P NMR signal at 18.9 ppm to the ^{1}H signals at 2.19 and 2.90 ppm.
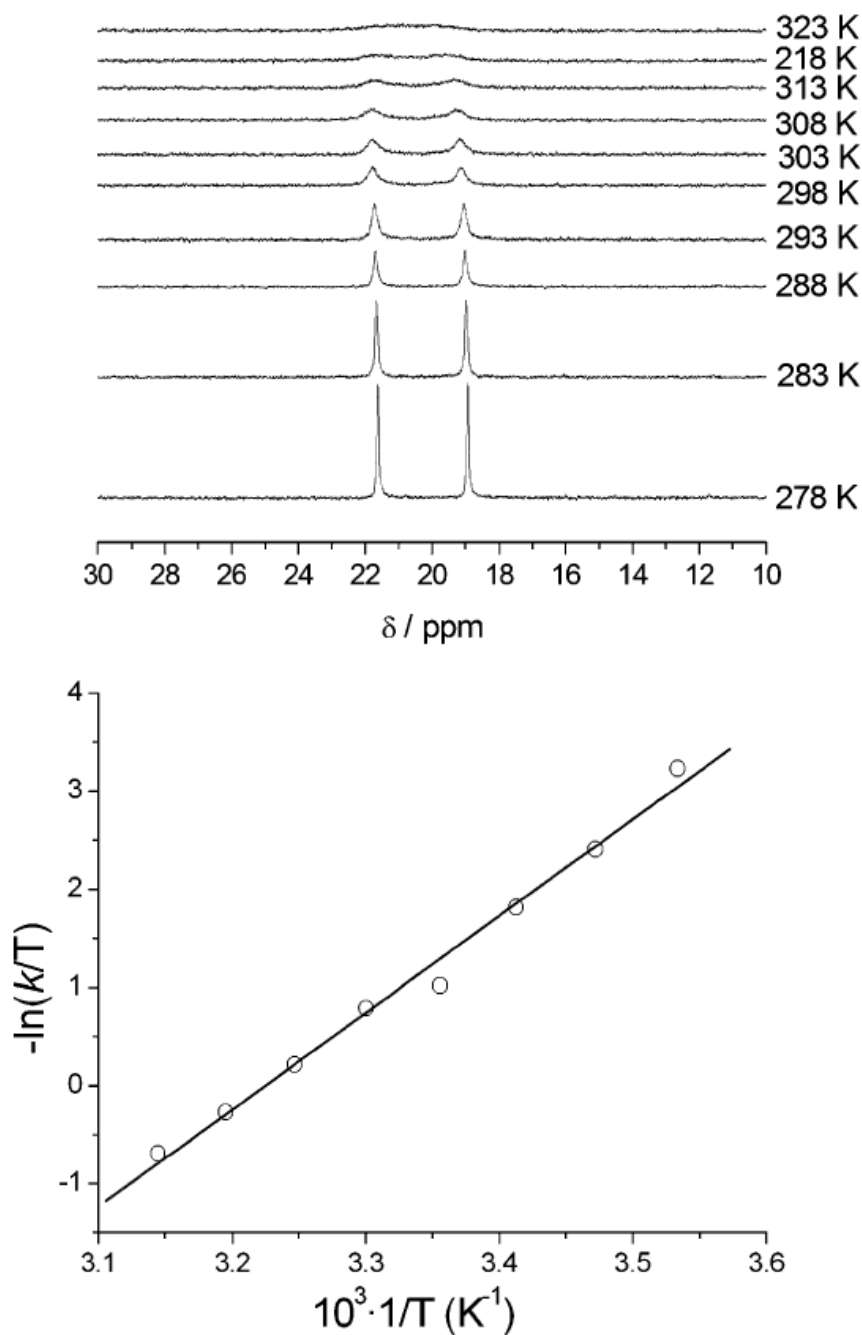
Figure 4. Top: ^{31}P-{H} NMR spectra of Lu**L**[4] recorded in D_2O solution at different temperatures (pD 10.9); see Scheme 1 for H labeling. Bottom: Eyring plot for the $\Delta \leftrightarrow \Lambda$ enantiomerization in Lu**L**[4] based upon line-broadening data.

The ^{1}H and ^{31}P spectra of Lu**L**[4] reflect the occurrence in solution of a conformational exchange process that can be attributed to a rotation of the methylenephosphonate groups leading to the $\Delta \leftrightarrow \Lambda$ enantiomerization mechanism previously observed with tetracarboxylated chelates.[26] The rotation of the methylenephosphonate groups exchanges the in-plane and out-of-plane methylenephosphonate groups (Scheme 2). This process is fast on the ^{31}P NMR time scale at room temperature in the case of the La[III] complex, and slow in the case of the Lu[III] analogue. Thus, there is an increasing rigidity of the complexes in solution on decreasing the ionic radius of the metal ion, as often observed for Ln[III] complexes due to the increased positive charge density of the lanthanide ion along the series.[27] The ^{1}H NMR spectra of the La[III] complex indicate that the $\Delta \leftrightarrow \Lambda$ enantiomerization process occurs through an intramolecular

mechanism that does not require the decoordination of methylenephosphonate groups, as such process would average the signals due to the geminal H5a and H5b protons. Indeed, the ^{1}H NMR spectra of the La^{III} and Lu^{III} complexes shows that the Δ↔Λ interconversion leads to the exchange of protons H5a(*ip*)↔H5a(*op*) and H5b(*ip*)↔H5b(*op*). A similar intramolecular Δ↔Λ interconversion has been observed for different Fe^{II}, Ni^{II} and Zn^{II} EDTA and EDTA-like complexes.[28]

A band-shape analysis was carried out on the ^{31}P resonances of Lu**L**^{4} over the 278–323 K temperature range in order to calculate the activation parameters for the Δ↔Λ interconversion process.

An Eyring plot (R^2> 0.995, Figure 4) of ln(k/T) versus $1/T$ [$k=\chi(k_bT/h)exp(\Delta S^{\#}/R-\Delta H^{\#}/RT)$, where $\chi$is the transmission coefficient assumed to be 1, k_b is the Boltzmann constant, T is the absolute temperature, k is the rate constant, and $\Delta G^{\#}$, $\Delta H^{\#}$, and $\Delta S^{\#}$ are the activation free energy, enthalpy, and entropy, respectively] yields the following activation parameters: $\Delta G^{\#}$=68.7±10.2 kJ mol^{-1} at 298 K, $\Delta H^{\#}$=81.9±3.3 kJ mol^{-1}, and $\Delta S^{\#}$=66.7±11.7 J K^{-1} mol^{-1}. The positive activation entropy obtained for the Δ↔Λ racemization in [Lu**L**^{4}] is probably related to a reorganization of the second-sphere hydration shell around the negatively charged oxygen donor atoms in the transition state. Positive $\Delta S^{\#}$ values have been recently reported for the arm rotation process occurring in Ln^{III}–DOTA analogues with methylenephosphonate pendant arms.[29]

Aiming to obtain information on the solution structure and dynamics of the Ln**L**^{4} complexes, we performed density functional theory (DFT) calculations at the B3LYP level. Different studies have demonstrated that, due to their charge and important structure ordering effect, phosphonate groups have a tendency to induce a well-defined second hydration sphere around the metal complexes.[12b, 30, 31] Thus, in our calculations we have taken into account solvent effects (water) by using a polarizable continuum model (PCM). Our previous calculations performed on the Gd**L**^{4} complex[4b] included a coordinated water molecule, in line with the relaxivity values and ^{17}O NMR shifts obtained for this complex (see below), and with the luminescence lifetimes measured for the Eu^{III} and Tb^{III}analogues. In the case of Lu^{III}, the presence of a coordinated water molecule cannot be tested with any of these methods, but the smaller ionic radius of the metal ion might result in a q=0 complex. For this reason, and to simplify the computational study, we did not include an explicit water molecule in our Lu**L**^{4} model system.

The minimum energy conformation calculated for Lu**L**^{4} is shown in Figure 5, while the bond lengths of the metal coordination environment are given in Table S2 (Supporting Information). According to our calculations the ligand provides an asymmetrical coordination of the metal ion, in contrast to the effective C_2 symmetry of the complex observed by NMR. A close inspection of the optimized geometry of Lu**L**^{4} shows that the asymmetrical coordination environment around Lu^{III} is due to a different orientation of the methylenephosphonate groups attached to one of the amine N atoms with respect to those bonded to the second one.

Indeed, the conformation adopted by the ligand in this complex results in the occurrence of two helicities: one associated with the layout of the methylenephosphonate arms (absolute configuration Δ or Λ, and the other with the four five-membered chelate rings formed by the binding of the N-CH$_2$-P-O units (each of them showing absolute configuration δ or λ).[32] The minimum energy conformation calculated for Lu**L**^{4} corresponds to the Δ(δλδλ) [or Λ(λδλδ)] form. The inversion of the two methylenephosphonate groups attached to one of the nitrogen atoms leads to a second energy minimum that shows an undistorted C_2 symmetry and corresponds to the Δ(δδδδ) [or Λ(λλλλ)] form. The calculated relative free energy of the Δ(δλδλ) conformation with respect to the Δ(δδδδ) one amounts to −10.3 kJ mol^{-1}. According to our calculations the interconversion between the Δ(δλδλ) and Δ(δδδδ) forms of the Lu^{III} complex is a one-step process involving the simultaneous inversion of two five-membered chelate rings (Figure 5). The free energy barrier associated with this process is relatively low, amounting only to 39.7 kJ mol^{-1}. The inversion of two five-membered chelate rings of the Δ(δδδδ) conformation may occur through the rotation of the two methylenephosphonate groups attached to either of the amine N atoms of the ligand, providing either the

starting $\Delta(\delta\lambda\delta\lambda)$ form or the equivalent $\Delta(\lambda\delta\lambda\delta)$ structure through transition states with identical energy (TS2 and TS2′ in Figure 5). Thus, most likely the LuL^4 complex adopts an asymmetrical $\Delta(\delta\lambda\delta\lambda)$ [or $\Lambda(\lambda\delta\lambda\delta)$] conformation in aqueous solution, a fast $\Delta(\delta\lambda\delta\lambda) \leftrightarrow \Delta(\delta\delta\delta\delta) \leftrightarrow \Delta(\lambda\delta\lambda\delta)$ rearrangement being responsible for the effective C_2 symmetry observed in the NMR spectra (C_2-averaging in Figure 5).

The transition state responsible for the $\Delta(\delta\lambda\delta\lambda) \leftrightarrow \Lambda(\lambda\delta\lambda\delta)$ enantiomerization process in LuL^4 is shown in Figure 5 (TS1). This process requires an important deformation of the Lu^{III} coordination environment enforced by the simultaneous rotation of the four methylenephosphonate groups. In particular the Lu-N distances experience an important lengthening on going from the ground to the transition state (from ca. 2.74 and 2.65 Å in the ground state to 2.82 Å in the TS). The calculated activation free energy for the $\Delta(\delta\lambda\delta\lambda)\leftrightarrow\Lambda(\lambda\delta\lambda\delta)$ interconversion process amounts to 71.9 kJ mol^{-1}. This value is in excellent agreement with that obtained experimentally (68.7 kJ mol^{-1}, see above), which supports that the mechanism predicted by our DFT calculations is basically correct.
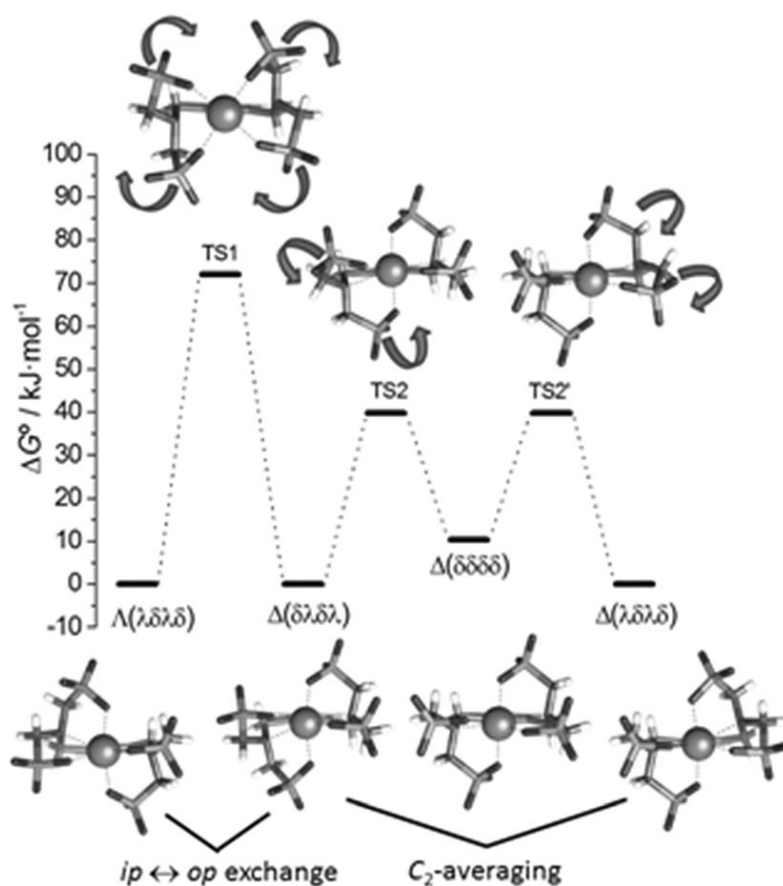

Figure 5. Relative free energies of minima, intermediates and transition states involved in the $\Delta(\delta\lambda\delta\lambda) \leftrightarrow \Delta(\delta\delta\delta\delta)$ and $\Delta(\lambda\delta\lambda\delta) \leftrightarrow \Lambda(\delta\lambda\delta\lambda)$ interconversion processes of LuL^4 in aqueous solution.

^{1}H Relaxivity and ^{17}O NMR Studies

Relaxivity (r_{1p}) represents the efficiency of the paramagnetic metal chelate in catalyzing the solvent nuclear magnetic relaxation at a given frequency and temperature, and it is defined as the increase of the water proton longitudinal relaxation rate (R_1) value normalized to a 1 mM concentration of the metal ion. Figure 6 represents the evolution of the relaxivity of the complexes as a function of the pH in water at 25 °C and 20 MHz. The relaxivity of GdL^4 measured at pH 10.5 (20 MHz and 298 K) increases smoothly from 7.7 to 8.9

mM^{-1} s^{-1} upon decreasing the pH at 6.5. In this pH range, extrapolation of the potentiometric data extracted for Eu (see Figure S4 for a distribution diagram of the [EuL^4] species as a function of pH) suggests that none or a single phosphonate group of the ligand are protonated, and these different protonated states likely have a significant impact on some of the physicochemical parameters that control proton r_{1p}. For instance, decreasing the negative electric charge of the complex is likely to induce a shortening of the distance between the Gd^{III} ion and proton nuclei of the coordinated water molecule, r_{Gd-H}, because of an increased electrostatic interaction between the coordinated water molecule and the metal ion. Below pH ~6.5, r_{1p} suddenly increases reaching a value of 20.0 mM^{-1} s^{-1} at pH 3.4. To unravel a possible change in hydration state of the complexes as a function of the pH, a titration was performed in which the excited state lifetime of the EuL^4 complex (assumed to be isostructural to the GdL^4 complex) was monitored as a function of the pH on water. The results (Table S3) did not indicate a drastic change of the hydration number within the pH range 2.7–11.5 and substantiate the hypothesis of aggregation phenomena as previously observed for other molecular Ln complexes.[33]
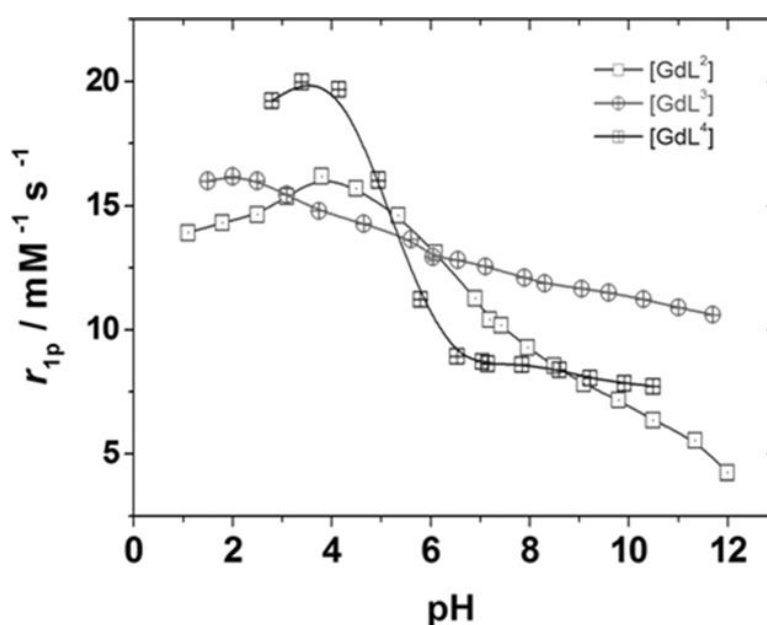

Figure 6. Plot of the relaxivity (20 MHz; 25 °C) measured for the Gd^{III} complexes investigated in this work as a function of pH. The solid lines are simply a guide for the eye.

The relaxivity of GdL^3 increases steadily on decreasing the pH from 11.7 (r_{1p}=10.6 mM^{-1} s^{-1} at 20 MHz and 298 K) to pH 2.0 (r_{1p}=16.2 mM^{-1} s^{-1}). This can be explained by the gradual protonation of phosphonate groups on lowering the pH of the solution, which decreases the negative electric charge of the complex. As a result of the hexadentate nature of the ligand and the reduced negative charge of the complex, the Gd^{III} ions are coordinatively unsaturated. Thus, phosphonate groups can act as bridges between two Gd^{III} ions, resulting in the formation of [GdL^3]n aggregates.

The ^{1}H NMRD profiles recorded for GdL^3 at pH 6.47 and 8.05 confirm this hypothesis (Figure 7). They show a plateau at low field (0.01–1 MHz), where relaxivity receives a significant contribution from the electron spin relaxation time. Above about 1 MHz the relaxivity decreases, reaching a minimum at about 10 MHz. Above 10 MHz r_{1p} increases, giving rise to a broad peak around ~70 MHz. Above about 10 MHz, the inner sphere contribution to r_{1p} is largely determined by the residence lifetime of the inner-sphere water molecule(s) (τ_M) and the rotational correlation time (τ_R). The relaxivity increase observed in the region 10–60 MHz is characteristic of systems with relatively long τ_R values. Furthermore, this relaxivity at 70 MHz is

slightly higher at pH 6.47 than at pH 8.05, in line with a more extended aggregation of the [GdL³] complex upon lowering the pH of the solution.
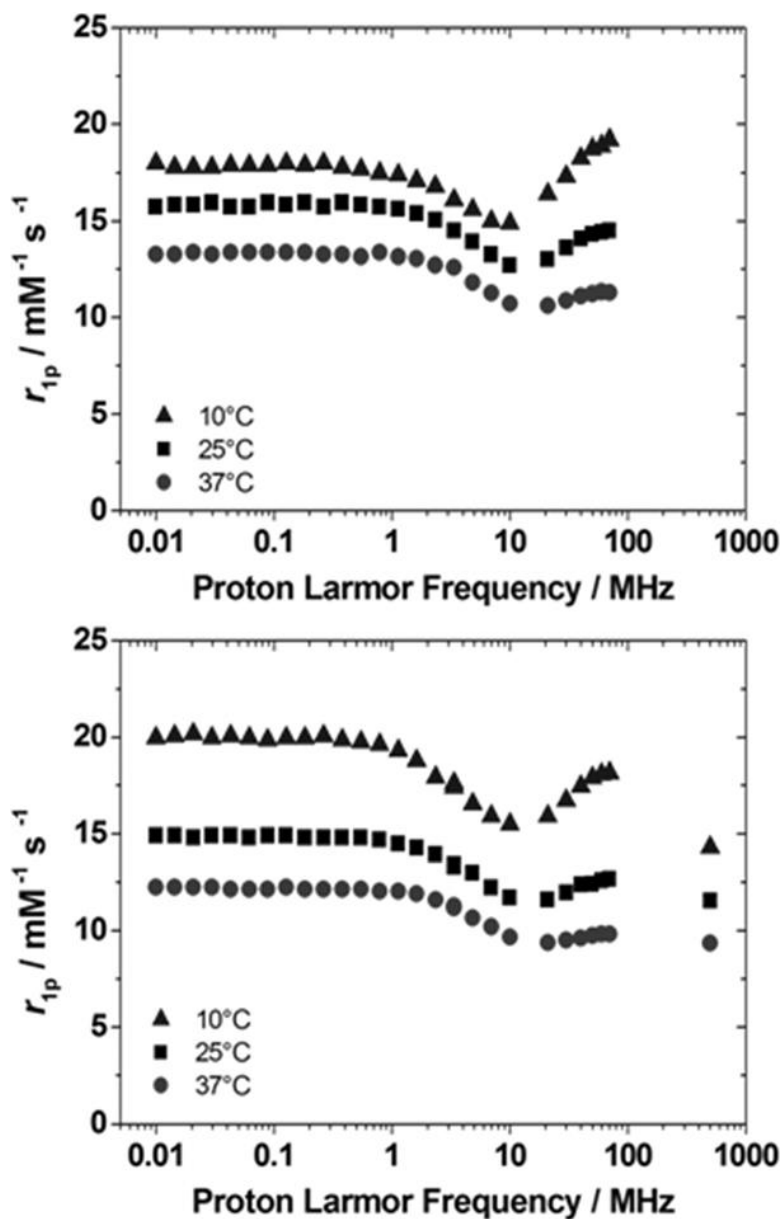

Figure 7. ¹H NMRD profiles recorded for GdL³ at pH 6.47 (top) and 8.05 (bottom).

The relaxivity of GdL² at 20 MHz and 298 K also increases on lowering the pH from 12.0 (r_{1p}=4.2 mM^{-1} s^{-1}) to 3.8 (r_{1p}=16.2 mM^{-1} s^{-1}), which again points to the formation of aggregates (Figure 6). The low relaxivity measured at pH 12.0 points to the absence of coordinated water molecules (q=0) at high pH values. This is probably related to the formation of hydroxo species and/or the coordination of carbonate anions dissolved in the aerated aqueous solution to the Gd^{III} ion, thereby replacing the bound water molecules.[34] The lower negative charge of GdL² compared with GdL³ and GdL⁴ may favors the formation of ternary adducts with carbonate. The ¹H NMRD profiles obtained at pH 11.8 and 7.1 (Figure S5) clearly confirm that lowering the pH favors both an increase of the hydration state and the formation of aggregates in solution. Indeed, at pH 7.1 r_{1p} increases in the frequency range 10-70 MHz, which is characteristic of slowly tumbling substrates.

The relaxivity increase is more pronounced that in the case of [GdL³], pointing to a more extended aggregation.

The NMRD profile recorded at 25 °C and pH 7.1 could be fitted assuming the following parameters: $q=1$, $\tau_R^{298}=290$ ps, $r=3.0$ Å, $\Delta^2=5\times10^{19}$ s^{-2} and $\tau_V=27$ ps (τ_v is the electronic correlation time for the modulation of the zero-field-splitting interaction and Δ^2 is the mean square zero-field-splitting energy). Although these parameters must be taken with caution, as both global and local motions might contribute to the τ_R in slowly tumbling substrates, the values obtained from this analysis are in agreement with the formation of relatively small aggregates (3–4 complex units). It must be pointed out that both the tendency to oligomerize and to increase the q value by going from basic to neutral/acidic conditions have been previously observed and reported in the case of other Gd^{III} phosphonate complexes.[35]

The GdL⁴ complex forms a monomeric species in solution with a well-defined hydration number ($q=1$) at about neutral pH. Thus, we have carried out a more detailed study of the parameters that govern the observed relaxivity. ¹H NMRD profiles of GdL⁴ were measured at 10, 25 and 37 °C in the proton Larmor frequency range 0.01–70 MHz at pH 7.4 (Figure 8).

The relaxivity of GdL⁴ decreases with increasing temperature over the entire range of proton Larmor frequency investigated, showing that the relaxivity is limited by the fast rotation of the complex in solution rather than by a slow water exchange rate. Furthermore, we have measured reduced transverse ¹⁷O relaxation rates ($1/T_{2r}$) and reduced ¹⁷O NMR chemical shifts ($\Delta\omega_r$) to obtain information on the exchange rate of the coordinated water molecule (Figure 8). The sign of the temperature dependence of $1/T_{2r}$ depends on whether the transverse relaxation is dominated by τ_M, which decreases with increasing temperature, or by the relaxation time of the bound water molecule, T_{2m}, which normally increases with increasing temperature. For GdL⁴, $1/T_{2r}$ decreases upon increasing temperature in the temperature range 352–274 K, which is typical of systems in the fast exchange regime ($k_{ex}^{298} > $ ca. 10^7 s^{-1}).

It has been demonstrated that phosphonate and phosphinate groups induce the formation of a second-sphere hydration shell around Gd^{III} complexes due to their high negative charge.[11a,36] Second-sphere water molecules remain a non-negligible time in the proximity of the Gd^{III} ion, thereby providing a significant contribution to the observed proton relaxivity.

The second-sphere term also contributes to the longitudinal ¹⁷O NMR relaxation, which is influenced by the dipolar and quadrupolar contributions, but not to the transverse ¹⁷O NMR relaxation and chemical shifts.[37, 38] Thus, a second-sphere contribution was taken into account only for the analysis of the ¹H NMRD data of GdL⁴. A simultaneous fitting of the ¹H NMRD and ¹⁷O NMR data was performed by using the Solomon-Bloembergen-Morgan theory to describe the inner- and second-sphere contributions to relaxivity,[39] the Freed model equations to account for the outer-sphere contribution to relaxivity,[40] and the Swift–Connick equations to represent the temperature dependence of ¹⁷O transverse relaxation rates and chemical shifts.[41] The following parameters have been fixed during the fitting procedure: the number of water molecules in the inner coordination sphere of Gd^{III} was fixed to $q=1$ on the basis of luminescence lifetime measurements; the distance between the proton nuclei of the coordinated water molecule and the Gd^{III} ion (r_{GdH}) was fixed at 3.0 Å,[42] while the distance of closest approach for the outer-sphere contribution, a_{GdH}, was set to 4.0 Å; the distance of second-sphere water protons and the Gd^{III} ion was fixed at 3.60 Å,[38] while the number of second-sphere water molecules was taken as $q^{2nd}=4$ and the residence time of these water molecules in the second hydration shell was set to 1 ns;[43] the values of the diffusion coefficient (D_{GdH}^{298}) and its activation energy (E_D) were fixed at the common values of 2.24×10^{-5} cm^2 s^{-1} and 21 kJ mol^{-1}, respectively.[44] Finally, the activation energies for the rotational correlation time, E_R, and the activation energy for the modulation of the zero-field-splitting (E_V) were fixed to typical values (18 and 1 kJ mol^{-1}, respectively). An excellent fit of the ¹H NMRD and ¹⁷O NMR data was obtained with the

parameters listed in Table 3, which also shows data reported previously for related non-macrocyclic systems containing phosphonate groups (see Scheme 3).

The sum of the outer-sphere and second-sphere contributions to relaxivity obtained from the fit of the NMRD and ^{17}O NMR data assumes the value of 4.9 mM^{-1} s^{-1} (298 K, 20 MHz). This value is quite comparable to the relaxivity observed for GdEGT4P (5.3 mM^{-1} s^{-1}), which contains four phosphonate groups but lacks any coordinated water molecule (the observed relaxivity is therefore the result of the outer-sphere and second-sphere mechanisms). The value of τ_R^{298} (121 ps) is in the range expected for a complex with low molecular weight, being very close to that reported for the complex of BCPE2P. The value obtained for the hyperfine coupling constant ($A/\hbar$) falls within the range reported for Gd^{III} complexes, which confirms the presence of one water molecule in the inner-sphere coordination shell of Gd^{III}.[45]
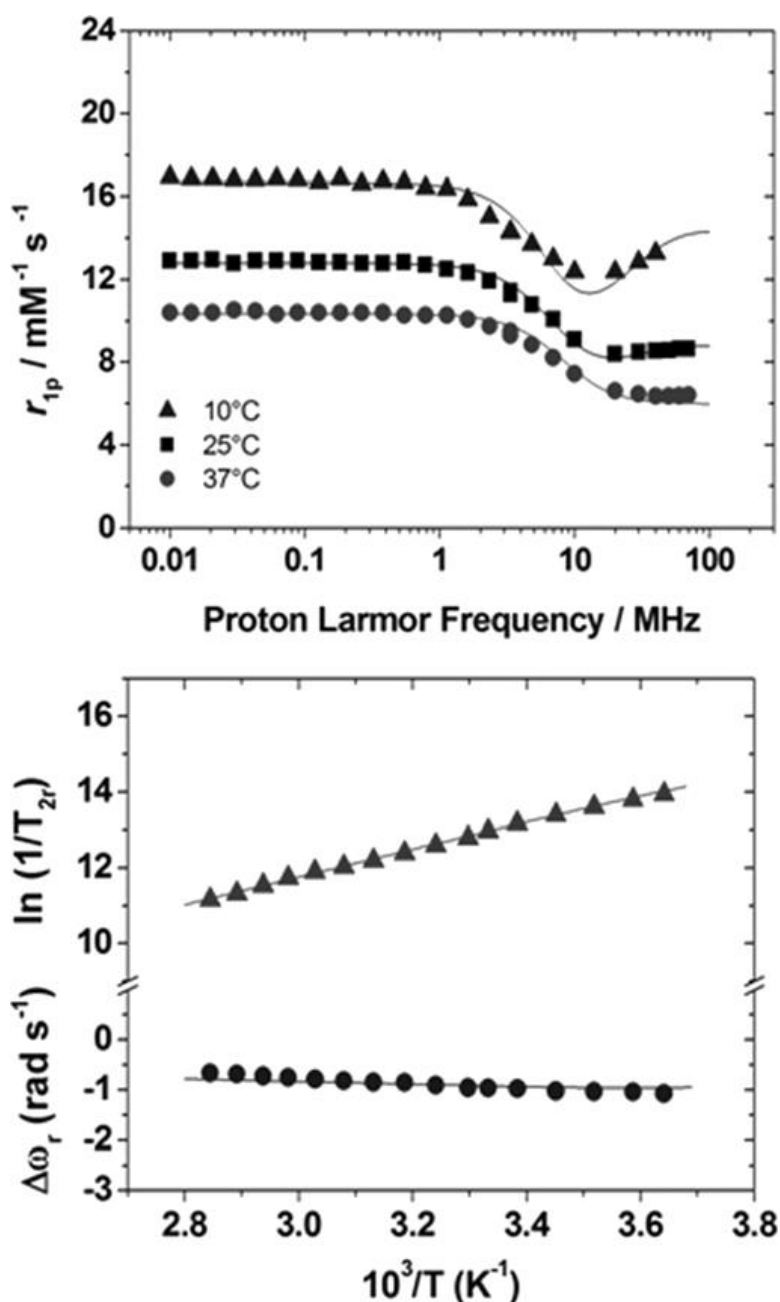

Figure 8. ^{1}H NMRD profiles (top) and reduced transverse ^{17}O relaxation rates (triangles) and ^{17}O chemical shifts (circles, bottom, 11.74 T) measured for Gd**L^4** at pH 7.4. The lines represent the fit of the data (see text).
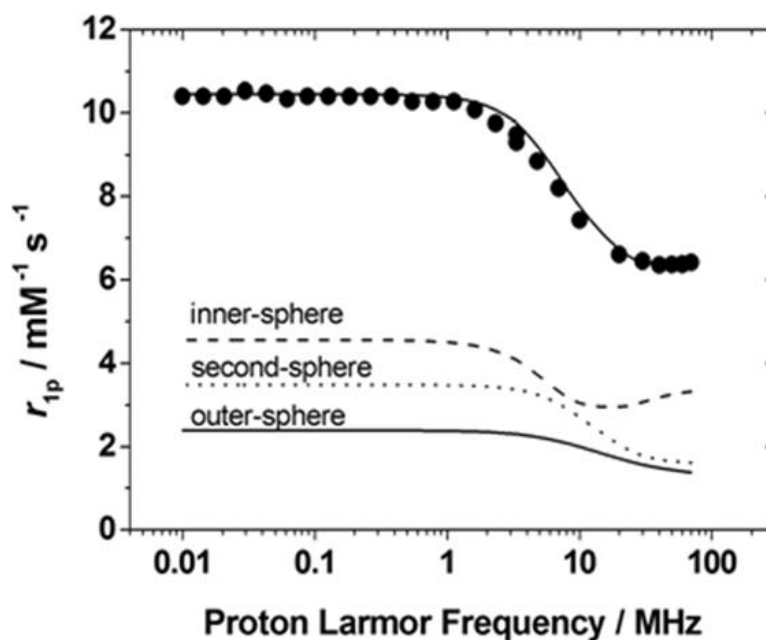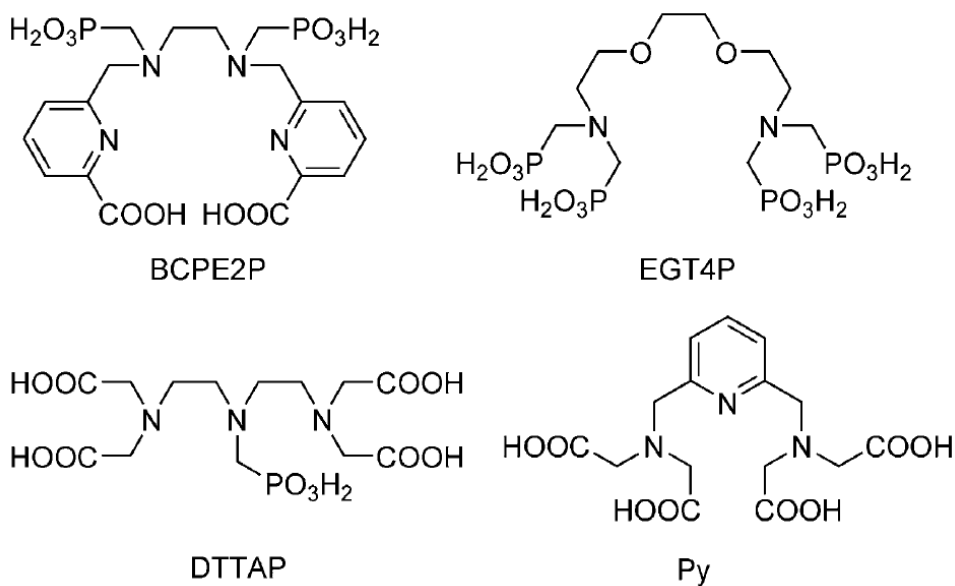
Figure 9. ^{1}H NMRD profile measured for Gd**L**[4] at pH 7.4 and 37 °C and the contributions of the inner-sphere, second-sphere and outer-sphere mechanisms obtained from the analysis of the data. The line through the experimental data points represents the fit of the data as described in the text.

Scheme 3. Ligands used for the comparison of relaxivity properties.

The parameters describing electron spin relaxation (Δ^2 and τ_V) are also close to those determined for related systems (Table 3). The exchange rate of the inner-sphere water molecule is very high when compared to those of [Gd(DTPA)]$^{2-}$ and [Gd(DOTA)]$^-$ (k_{ex}^{298}=3.3×10^6 and 4.1×10^6 s^{-1}, respectively),[44] and about 15 times faster than that reported for the complex of the carboxylate derivative Py (Scheme 2). This is in line with previous observations, which showed that the replacement of acetate groups by phosphonate units results in a marked acceleration of the exchange rate of inner-sphere water molecules.[48]

As stated before, a number of assumptions had to be made to account for the second-sphere contribution to relaxivity. Thus, the contributions calculated for the inner- second- and outer-sphere mechanisms from the analysis of the NMRD profiles have to be taken with some caution. In spite of this, our analysis suggests that the contribution of the second-sphere mechanism to the overall relaxivity at physiological temperature is quite important (Figure 9). At low fields (0.01–10 Hz) this contribution is clearly higher than that of the outer-sphere, while at higher fields the second- and outer-sphere mechanisms provide comparable contributions to the overall relaxivity.

Table 3. Parameters obtained from the simultaneous analysis of ^{1}H NMRD profiles and ^{17}O NMR data (11.74 T) for the Gd^{III} complex of $\mathbf{L^4}$ and the related ligands.

Parameter	$\mathbf{L^4}$	EGT4P[b]	BCPE2P[c]	DTTAP[d]	Py[e]
$^{20}r_1^{298}$ [mM^{-1} s^{-1}]	8.4	5.3	4.9	6.5	
$\Delta^2 \times 10^{19}$ [s^{-2}]	9.2±0.5	6.2	8.2	4.5	9.6
τ_V^{298} [ps]	15±1	23	22	22	2.8
$k_{ex}^{298} \times 10^6$ [s^{-1}]	142.8±0.5	/	700	11.4	9.3
τ_R^{298} [ps]	121±4	/	109	86	92
q	1[a]	0	0.64	1.0	2
r_{GdH} [Å]	3.0[a]	/	3.1	3.1	–
q^{2nd}	4	4	3	2.2	–
r_{GdH}^{2nd} [Å]	3.60	3.82	3.5	3.5	–
E_V [kJ mol^{-1}]	1.0[a]		1.0	1.0	1.0
$\Delta H_M^{\#}$ [kJ mol^{-1}]	29.5±0.6	/	22	41	50.4
$A/\hbar \times 10^6$ [rad s^{-1}]	−3.5±0.2	/	−3.5	−3.3	−3.7

[a] Parameters fixed during the fitting procedure.
[b] Data from reference [46].
[c] Data from reference [37].
[d] Data from reference [30].
[e] Parameters obtained from the analysis of ^{17}O NMR data, reference [47].

Mouse imaging

Considering the excellent relaxivity properties of the Gd^{III} complex of ligand $\mathbf{L^4}$, it was of particular interest to check its properties in vivo. The complex was injected through the tail vein of a mice and its biodistribution was followed as a function of time in different regions of interest (ROI) over a period of 10 min post-injection. The ROIs correspond to the relaxivity variations for muscles, kidneys (left and right), liver and vein and are presented in Figure S5. Figure 10 displays images acquired before and 120 min post injection, while the variations of the relaxivity in the ROI as a function of time are shown in Figure 11.

As can be seen from Figure 11, the complex shows a rapid clearance from blood, with a signal enhancement of the different tissues. Contrast is, at maximum, increased by about 30 % in kidney, 25 % in vein, 10 % in liver and muscle. In this last tissue, the contrast decreased slowly during the 10 min of acquisition. Elimination is mainly observed by the kidneys. Blood clearance was unfortunately too rapid to envisage angiography. During the course of the experiment, it should be emphasized that the administration seemed to be particularly well tolerated by the animal with no movements during injection, a normal wakening, and no sign of a delayed intolerance (neither thirsty, nor behavioral abnormalities).
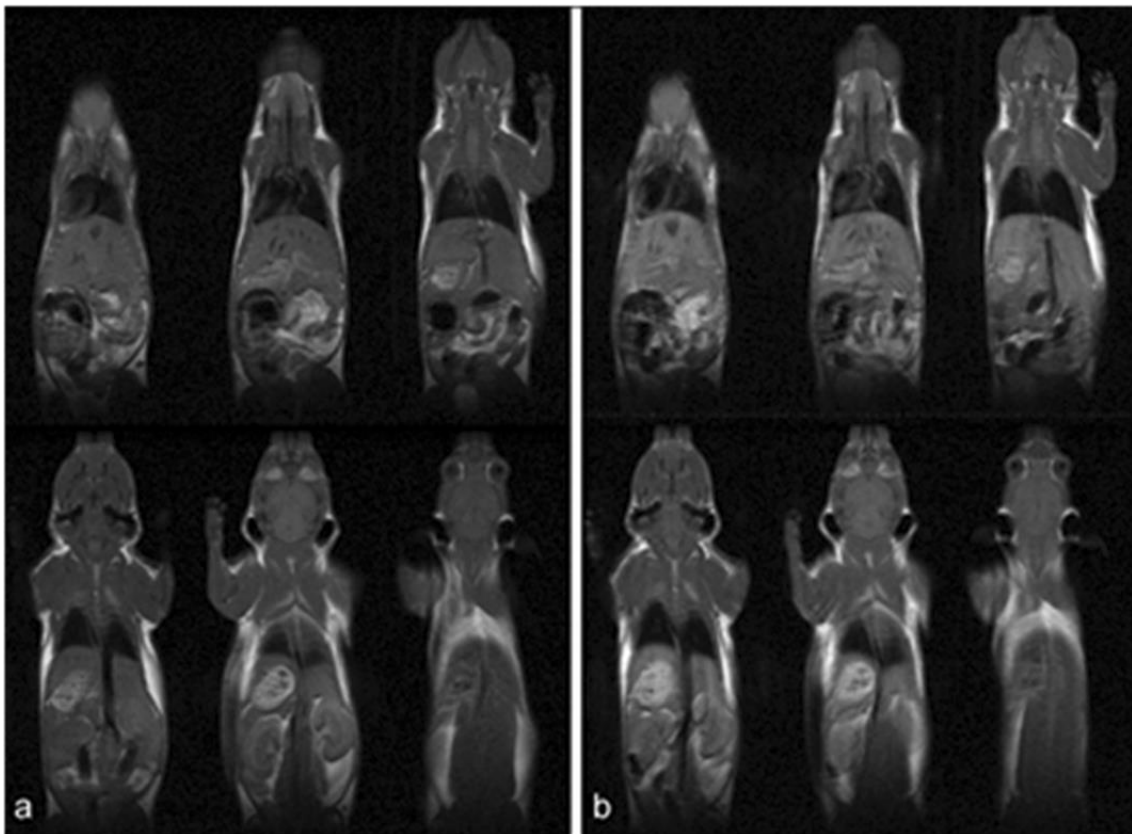
Figure 10. Different slices of a mouse MRI imaging observed before (a) and 120 min (b) post-injection of 200 μL of a GdL^4 solution at 200 μL min^{-1} (0.02 mmol Gd per kg).
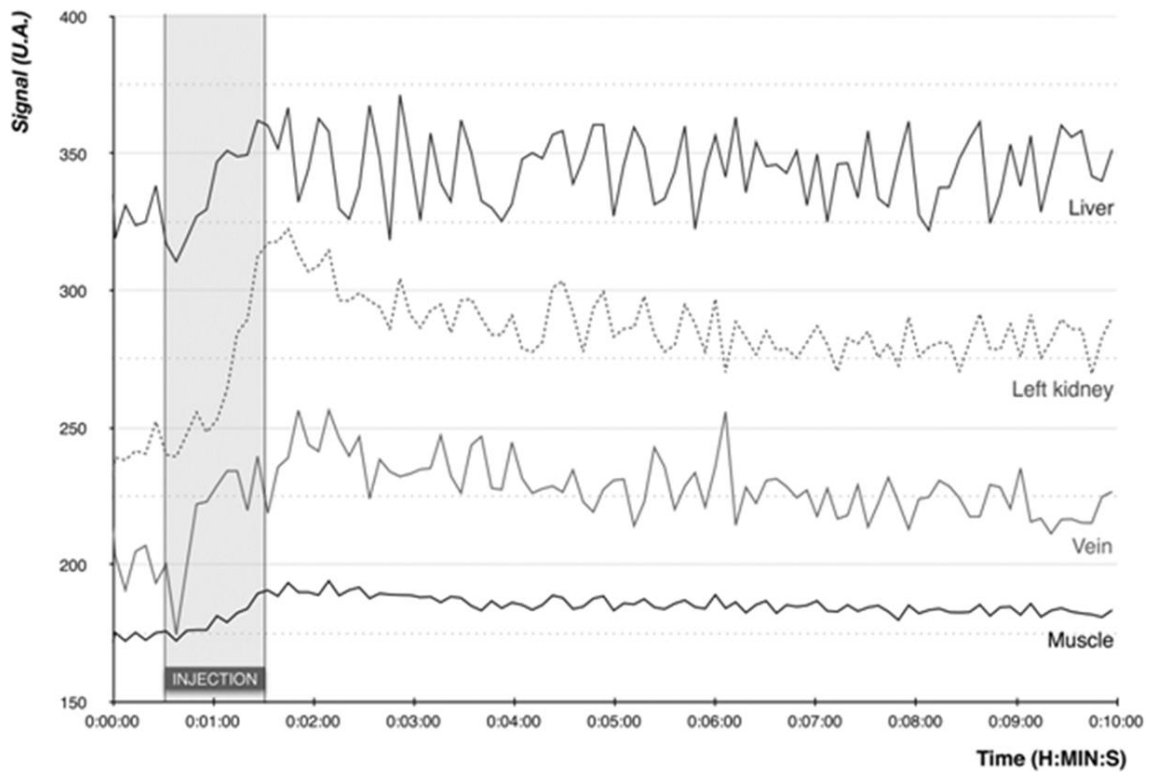

Figure 11. Relaxivity variations observed in the regions of interest during the biodistribution experiment.

Conclusion

Pyridyl-based phosphonated chelates represent very promising platforms for the complexation of lanthanide cations. In particular, the complexes obtained with the tetraphosphonated ligand L^4 forms complexes with an extremely high thermodynamic stability. Nevertheless, the presence of numerous phosphonate functions is also accompanied by important secondary interactions, probably related to hydrogen-bonding interactions, especially in acidic media. For the Gd^{III} complexes studied here, these interactions are translated into important contributions of the second and outer sphere mechanisms to the overall relaxivity of the compounds. Additionally, the decrease of the pH led to the formation of aggregates which severely impacts the rotational correlation times and led to further increase of the relaxivity. MRI imaging on mice showed the GdL^4 complex to be well suited for contrast enhancement, while small modifications on the ligand backbone such as *para*-functionalisation of the central pyridine ring[49] may allow an increase of the retention time in the bloodstream. Finally, although yet only superficially understood, the formation of these aggregates or polymeric species may correspond to discrete entities, as suggested by the results of the UV/Vis titration experiments (Figure 1 and S1) and as observed for other phosphonated[50] and carboxylated[51] ligands. Current efforts are directed towards the understanding of these Ln^{III} based supramolecular assemblies through mixtures of different luminescent lanthanide complexes and the study of Ln^{III} to Ln^{III} energy transfer phenomena.[52]

Experimental Section

Ligands L^2 to L^4 were synthesized according to previously published procedure.[18]

Potentiometric titrations: Full experimental details can be found in the supplementary information section.

Spectroscopy: UV/Vis absorption spectra were recorded on a Specord 205 (Analytik Jena) or a Perkin–Elmer lambda 950 spectrometer. Steady-state luminescence emission and excitation spectra were recorded on a Horiba Jobin Yvon Fluorolog 3 spectrometer working with a continuous 450 W Xe lamp. Detection was performed with a Hamamatsu R928 photomultiplier. All spectra were corrected for the instrumental response. When necessary, a 399 nm cut off filter was used to eliminate the second order artefacts. Phosphorescence decays were measured on the same instrument working in the phosphorescence mode, with 50 µs delay time and a 100 ms integration window or working in the Time Correlated Single Photon Counting (TCSPC) Lifetime Spectroscopy mode, both using a Xenon flash lamp as the excitation source. Monoexponential decay profiles were fitted with the FAST program from Edinburgh Instruments or with the Data station software from Jobin Yvon. Luminescence quantum yields were measured according to conventional procedures, with optically diluted solutions (optical density <0.05), using rhodamine 6G in water (ϕ=76.0 %)[53] or a Tb^{III} complex of the literature (ϕ=31.0 %)[54] as references for Tb^{III} and $[Ru(bipy)_3]Cl_2$ in water (ϕ=4.0 %)[55] for Eu^{III}. Estimated errors are ±15 %.

NMR measurements: ^1H, ^{13}C and ^{31}P NMR spectra were recorded in D_2O on a Bruker Avance 300 MHz spectrometer operating at 300.13 (^1H), 75.47 (^{13}C) and 121.49 MHz (^{31}P). Spectral assignments were based in part on two-dimensional COSY, NOESY, HMQC, and HMBC experiments. ^1H, ^{13}C NMR spectra recorded in D_2O solution were referenced by using *tert*-butyl alcohol as an internal standard with the methyl signal calibrated at δ=1.2 (^1H) and 31.2 ppm (^{13}C). ^{31}P NMR chemical shifts were reported in ppm relative to external H_3PO4 (85 %). Samples of the complexes for NMR measurements were prepared by dissolving equimolar amounts of the ligand and hydrated $LnCl_3$ in D_2O, followed by adjustment of the pH with ND₄OD and DCl (Aldrich) solutions in D_2O. Values of pD are corrected for deuterium isotopic effect (pD=pH$_{reading}$ + 0.4).[56]

The water proton longitudinal relaxation rates as a function of temperature (20 MHz) were measured with a StelarRelaxometer (Mede, PV, Italy) on about 0.6–2.0 mM aqueous solutions in non-deuterated water. The exact Gd^{III} concentrations were determined by measurement of bulk magnetic susceptibility shifts of a tBuOH signal on a Bruker Avance III spectrometer (11.74 T).[57] The ^{1}H T_1 relaxation times were acquired by the standard inversion recovery method with typical 90° pulse width of 3.5 µs, 16 experiments of 4 scans. The reproducibility of the T_1 data was ±5 %. The temperature was controlled with a Stelar VTC-91 airflow heater equipped with a calibrated copper-constantan thermocouple (uncertainty of ±0.1 °C). The proton $1/T_1$ NMRD profiles were measured on a fast field-cycling Stelar Smart Tracer relaxometer over a continuum of magnetic field strengths from 0.00024–0.25 T (corresponding to 0.01–10 MHz proton Larmor frequencies). The relaxometer operates under computer control with an absolute uncertainty in $1/T_1$ of ±1 %. Additional data points in the range 15–70 MHz were obtained on a Stelar Relaxometer equipped with a Bruker WP80 NMR electromagnet adapted to variable-field measurements (15–80 MHz proton Larmor frequency).^{17}O NMR measurements were recorded on a Bruker Avance III spectrometer (11.74 T) equipped with a 5 mm probe and standard temperature control unit. A 12.3 mM aqueous solution of Gd**L^4** containing 1.0 % of the ^{17}O isotope (CortecNet, Paris) was used. The observed transverse relaxation rates were calculated from the signal width at half-height.

DFT calculations: All calculations were performed employing hybrid DFT with the B3LYP exchange-correlation functional,[58, 59] and the Gaussian 09 package (Revision B.01).[60] Full geometry optimizations of the [Lu**L^4**]$^{5-}$ systems were performed in aqueous solution by using the large-core effective core potential (LCECP) of Dolg et al. and the related [5s4p3d]-GTO valence basis set for the lanthanides,[61] and the 6-31G(d) basis set for C, H, N, O and P atoms. No symmetry constraints have been imposed during the optimizations. The default values for the integration grid ("fine") and the SCF energy convergence criteria (10^{-8}) were used. The stationary points found on the potential energy surfaces as a result of the geometry optimizations were checked to correspond to energy minima rather than saddle points using frequency analysis. Solvent effects were evaluated by using the integral equation formalism of the polarizable continuum model (IEFPCM), as implemented in Gaussian 09.[62]

The relative free energies of the different conformations obtained from geometry optimizations were calculated in aqueous solution at the B3LYP/LCECP/6-31G(d) level, including non-potential-energy contributions (zero point energies and thermal terms) obtained through frequency analysis. The $\Delta(\delta\lambda\delta\lambda) \leftrightarrow \Delta(\delta\delta\delta\delta)$ and $\Delta(\delta\lambda\delta\lambda) \leftrightarrow \Lambda(\delta\lambda\delta\lambda)$ interconversion processes were investigated using the synchronous transit-guided quasi-Newton method.[63] The nature of the saddle points was characterized by frequency analysis (one imaginary frequency). Examination of the normal mode corresponding to the imaginary frequency confirmed that the corresponding transition state connects the reactant and product of interest. In the case of the $\Delta(\delta\lambda\delta\lambda) \leftrightarrow \Lambda(\delta\lambda\delta\lambda)$ interconversion processes this was further confirmed by following the reaction path by integrating the intrinsic reaction coordinate (IRC).[64] The calculated free energy barriers include non-potential energy contributions obtained by frequency analysis.

NMR shielding tensors were calculated in aqueous solution by using the GIAO[65] method and the more extended 6-311G(d,p) basis set for the ligand atoms. The calculated absolute chemical shielding values (σ_{iso}) were converted to chemical shifts (δ) relative to 85 % H_3PO_4 by comparison to the chemical shielding of PH_3 at the same level of theory.[66]

$$\delta_{calcd}\left([Lu\mathbf{L^4}]^{5-}\right) = \sigma_{calcd}(PH_3) - \sigma_{calcd}\left([Lu\mathbf{L^4}]^{5-}\right) - 266.1$$

Mouse imaging: Mice whole body MR images were acquired at 1.5 T, using a preclinical MRI device (OPTImouse, RS2D, France), inside a volume RF coil (RapidBiomedical, Germany) of 40 mm in diameter. Intravenous administration of the contrast agent was performed via a catheter in a tail vein of the mice (three animals, mean weight 25 g), connected to an infusion pump (PHD 2000, Harvard Apparatus, USA) at a speed of 200 µL min^{-1} (total volume of 200 µL, including 100 µL of contrast agent at 5 mM, corresponding to a Gd dose of 0.02 mmol kg^{-1} per body weight). Mice were kept under anaesthesia (Isoflurane + air) and warmed to maintain homeostasis, throughout acquisition, in an imaging cell (Minerve, France). 2D dynamic acquisition (1 slice of 1.25 mm thickness) involves 100 images every 6 s for a total acquisition time of 10 min. Acquisition was started about 30 s before contrast agent injection beginning. Regions of interest (ROI) were drawn in Osirix (http://www.osirix-viewer.com/), encompassing part of liver, kidney, muscle and inferior vena cava. Mean values of signal inside these ROI were computed for all images leading to time-signal curves.

[1] a) C. F. G. C. Geraldes, S. Laurent, *Contrast Media Mol. Imaging* 2009, **4**, 1; b) S. Aime, M. Botta, E. Terreno, *Adv. Inorg. Chem.* 2005, **57**, 173; c) E. Boros, E. M. Gale, P. Caravan, *Dalton Trans.* **2015**, DOI: 10.1039/c4dt02958e; d) *The Chemistry of Contrast Agents in Medical Magnetic Resonance Imaging* (Eds.: A. E. Merbach, L. Helm, É. Tóth), 2nd ed., Wiley, Chichester (UK), 2013.

[2] a) J. L. Major, T. J. Meade, *Acc. Chem. Res.* 2009, **42**, 893; b) T. Chauvin, P. Durand, M. Bernier, H. Meudal, B.-T. Doan, F. Noury, B. Badet, J.-C. Beloeil, E. Toth, *Angew. Chem. Int. Ed.* 2008, **47**, 4370; *Angew. Chem.* 2008, **120**, 4442.

[3] J. Galezowskaa, E. Gumienna-Konteckab, *Coord. Chem. Rev.* 2012, **256**, 105.

[4] a) E. Boros, S. Karimi, N. Kenton, L. Helm, P. Caravan, *Inorg. Chem.* 2014, **53**, 6985; b) S. Abada, A. Lecointre, M. Elhabiri, D. Esteban-Gomez, C. Platas-Iglesias, G. Tallec, M. Mazzanti, L. J. Charbonnière, *Chem. Commun.* 2012, **48**, 4085.

[5] L. D. Freedman, G. O. Doak, *Chem. Rev.* 1957, **57**, 479.

[6] I. Lukeš, J. Kotek, P. Vojtı́sek, P. Hermann, *Coord. Chem. Rev.* 2001, **216–217**, 287.

[7] K. Nchimi Nono, A. Lecointre, M. Regueiro-Figueroa, C. Platas-Iglesias, L. J. Charbonnière, *Inorg. Chem.* 2011, **50**, 1689.

[8] a) C. F. G. C. Geraldes, A. D. Sherry, W. P. Cacheris, *Inorg. Chem.* 1989, **28**, 3336; b) K. P. Guerra, R. Delgado, L. M. P. Lima, M. G. B. Drew, V. Félix, *Dalton Trans.* 2004, 1812; c) A. Nonat, M. Giraud, C. Gateau, P. H. Fries, L. Helm, M. Mazzanti, *Dalton Trans.* 2009, 8033.

[9] a) F. Benetollo, G. Bombieri, L. Calabi, S. Aime, M. Botta, *Inorg. Chem.* 2003, **42**, 148; b) M.-R. Spirlet, J. Rebizant, J.-F. Desreux, M.-F. Loncin, *Inorg. Chem.* 1984, **23**, 359.

[10] F. Avecilla, J. A. Peters, C. F. G. C. Geraldes, *Eur. J. Inorg. Chem.* 2003, 4179.

[11] a) S. Aime, E. Gianolio, D. Corpillo, C. Cavalotti, G. Palmisano, M. Sisti, G. B. Giovenzana, R. Pagliarin, *Helv. Chim. Acta* 2003, **86**, 615; b) S. Aime, M. Botta, S. Geninatti Crich, G. Giovenzana, R. Pagliarin, M. Sisti, E. Terreno, *Magn. Reson. Chem.* 1998, **36**, S200.

[12] a) F. K. Kálmán, M. Woods, P. Caravan, P. Jurek, M. Spiller, G. Tircso, R. Kiraly, E. Brucher, D. Sherry, *Inorg. Chem.* 2007, **46**, 5260; b) M. Botta, *Eur. J. Inorg. Chem.* 2000, 399–407.

[13] K. Nchimi-Nono, D. Wegner, S. Linden, A. Lecointre, L. Ehret-Sabatier, S. Shakir, N. Hildebrandt, L. J. Charbonnière, *Org. Biomol. Chem.* 2013, **11**, 6493.

[14] a) S. Abada, A. Lecointre, M. Elhabiri, L. J. Charbonnière, *Dalton Trans.* 2010, **39**, 9055; b) C. Christine, M. Koubemba, S. Shakir, S. Clavier, L. Ehret-Sabatier, F. Saupe, G. Orend, L. J. Charbonnière, *Org. Biomol. Chem.* 2012, **10**, 9183; c) S. Abada, A. Lecointre, I. Déchamps, C. Platas-Iglesias, C. Christine, M. Elhabiri, L. J. Charbonnière, *Radiochim. Acta* 2011, **99**, 663.

[15] S. I. Weissman, *J. Chem. Phys.* 1942, **10**, 214.

[16] A. Beeby, I. M. Clarkson, R. S. Dickins, S. Faulkner, D. Parker, L. Royle, A. S. de Sousa, J. A. G. Williams, M. Woods, *J. Chem. Soc. Perkin Trans. 2* 1999, 493.

[17] M. Regueiro-Figueroa, B. Bensenane, M. Rucsak, D. Esteban-Gomez, L. J. Charbonnière, G. Tyrsco, I. Toth, A. de Blas, T. Rodriguez-Blas, C. Platas-Iglesias, *Inorg. Chem.* 2011, **50**, 4125.

[18] S. Abada, A. Lecointre, C. Christine, L. Ehret-Sabatier, F. Saupe, G. Orend, D. Brasse, A. Ouadi, T. Hussenet, P. Laquerrière, M. Elhabiri, L. J. Charbonnière, *Org. Biomol. Chem.* 2014, **12**, 9601.

[19] G. D. Klungness, R. H. Byrne, *Polyhedron* 2000, **19**, 99.

[20] W. P. Cacheris, S. K. Nickle, A. D. Sherry, *Inorg. Chem.* 1987, **26**, 958.

[21] A. D. Sherry, J. Ren, J. Huskens, E. Brucher, E. Toth, C. F. G. C. Geraldes, M. M. C. A. Castro, W. P. Cacheris, *Inorg. Chem.* 1996, **35**, 4604.

[22] W. R. Harris, C. J. Carrano, K. N. Raymond, *J. Am. Chem. Soc.* 1979, **101**, 2213.

[23] P. Michelle Fitzsimmons, S. C. Jackels, *Inorg. Chim. Acta* 1996, **246**, 301.

[24] a) C. F. G. C. Geraldes, A. D. Sherry, G. E. Kiefer, *J. Magn. Reson.* 1992, **97**, 290; b) J. Brandel, A. Lecointre, J. Kollek, S. Michel, V. Hubscher-Bruder, I. Déschamps-Olivier, C. Platas-Iglesias, L. J. Charbonnière, *Dalton Trans.* 2014, **43**, 9070.

[25] a) G. Barone, L. Gomez-Paloma, D. Duca, A. Silvestri, R. Riccio, G. Bifulco, *Chem. Eur. J.* 2002, **8**, 3233; b) L. Vaiana, M. Regueiro-Figueroa, M. Mato-Iglesias, C. Platas-Iglesias, D. Esteban-Gomez, A. de Blas, T. Rodriguez-Blas, *Inorg. Chem.* 2007, **46**, 8271.

[26] a) M. Mato-Iglesias, T. Rodriguez-Blas, C. Platas-Iglesias, M. Starck, R. Ziessel, L. J. Charbonnière, *Inorg. Chem.* 2009, **48**, 1507; b) R. Negri, Z. Baranyai, L. Tei, G. B. Giovenzana, C. Platas-Iglesias, A. C. Benyei, J. Bodnar, J. A. Vagner, M. Botta, *Inorg. Chem.* 2014, **53**, 12499.

[27] a) C. Platas, F. Avecilla, A. de Blas, C. F. G. C. Geraldes, T. Rodríguez-Blas, H. Adams, J. Mahía, *Inorg. Chem.* 1999, **38**, 3190; b) G. Zucchi, R. Scopelliti, P.-A. Pittet, J.-C. G. Bünzli, R. D. Rogers, *J. Chem. Soc. Dalton Trans.* 1999, 931.

[28] a) J. Maigut, R. Meier, A. Zahl, R. van Eldik, *Inorg. Chem.* 2008, **47**, 5702; b) J. Maigut, R. Meier, A. Zahl, R. van Eldik, *Inorg. Chem.* 2007, **46**, 5361; c) R. Meier, C. Platas-Iglesias, F. W. Heinemann, G. Linti, J. Schulte, S. K. Srivastava, *Inorg. Chem.* 2014, **53**, 6684.

[29] M. Purgel, Z. Baranyai, A. de Blas, T. Rodríguez-Blas, I. Bányai, C. Platas-Iglesias, I. Tóth, *Inorg. Chem.* 2010, **49**, 4370.

[30] J. Kotek, P. Lebduskova, P. Hermann, L. Vander Elst, R. N. Muller, C. F. G. C. Geraldes, T. Maschmeyer, I. Luker, J. A. Peters, *Chem. Eur. J.* 2003, **9**, 5899.

[31] M. Mato-Iglesias, E. Valgo, C. Platas-Iglesias, E. Toth, A. de Blas, T. Rodríguez-Blas, *Dalton Trans.* 2006, 5404.

[32] a) E. J. Corey, J. C. Bailar Jr., *J. Am. Chem. Soc.* 1959, **81**, 2620; b) J. K. Beattie, *Acc. Chem. Res.* 1971, **4**, 253.

[33] M. Regueiro-Figueroa, A. Nonat, G. A. Rolla, D. Esteban-Gómez, A. de Blas, T. Rodríguez-Blas, L. J. Charbonnière, M. Botta, C. Platas-Iglesias, *Chem. Eur. J.* 2013, **19**, 11696.

[34] a) Z. Baranyai, M. Botta, M. Fekete, G. B. Giovenzana, R. Negri, L. Tei, C. Platas-Iglesias, *Chem. Eur. J.* 2012, **18**, 7680; b) C. Platas, F. Avecilla, A. de Blas, T. Rodríguez-Blas, C. F. G. C. Geraldes, E. Toth, A. E. Merbach, J.-C. G. Bünzli, *J. Chem. Soc. Dalton Trans.* 2000, 611.

[35] a) C. F. G. C. Geraldes, R. D. Brown 3rd, W. P. Cacheris, S. Koenig, A. D. Sherry, M. Spiller, *Magn. Reson. Med.* 1989, **9**, 94; b) J. Gałezowska, R. Janicki, A. Mondry, R. Burgada, T. Bailly, M. Lecouvey, H. Kozłowski, *Dalton Trans.* 2006, 4384.

[36] a) Z. Kotková, G. A. Pereira, K. Djanashvili, J. Kotek, J. Rudovsky, P. Hermann, L. VanderElst, R. N. Muller, C. F. G. C. Geraldes, I. Lukes, J. A. Peters, *Eur. J. Inorg. Chem.* 2009, 119; b) L. M. P. Lima, R. Delgado, P. Hermann, R. Sevcik, P. Lubal, H. F. Carvalho, A. F. Martins, E. Toth, C. F. G. C. Geraldes, *Eur. J. Inorg. Chem.* 2012, 2549; c) P. Hermann, J. Kotek, V. Kubicek, I. Lukes, *Dalton Trans.* 2008, 3027; d) J. Rudovsky, M. Botta, P. Hermann, A. Koridze, S. Aime, *Dalton Trans.* 2006, 2323; e) J. Rudovsky, J. Kotek, P. Hermann, I. Lukes, V. Mainero, S. Aime, *Org. Biomol. Chem.* 2005, **3**, 112.

[37] E. Balogh, C. Mato-Iglesias, C. Platas-Iglesias, E. Tóth, K. Djanashvili, J. A. Peters, A. de Blas, T. Rodríguez-Blas, *Inorg. Chem.* 2006, **45**, 8719.

[38] P. Lebduskova, P. Hermann, L. Helm, E. Toth, J. Kotek, K. Binnemans, J. Rudovsky, I. Luker, A. E. Merbach, *Dalton Trans.* 2007, 493.

[39] a) I. Solomon, *Phys. Rev.* 1955, **99**, 559; b) I. Solomon, N. Bloembergen, *J. Chem. Phys.* 1956, **25**, 261; c) N. Bloembergen, *J. Chem. Phys.* 1957, **27**, 572; d) N. Bloembergen, L. O. Morgan, *J. Chem. Phys.* 1961, **34**, 842.

[40] J. H. Freed, *J. Chem. Phys.* 1978, **68**, 4034.

[41] a) T. J. Swift, R. E. Connick, *J. Chem. Phys.* 1962, **37**, 307; b) T. J. Swift, R. E. Connick, *J. Chem. Phys.* 1964, **41**, 2553.

[42] a) A. M. Raitsimring, A. V. Astashkin, D. Baute, D. Goldfarb, P. Caravan, *J. Phys. Chem. A* 2004, **108**, 7318; b) A. V. Astashkin, A. M. Raitsimring, P. Caravan, *J. Phys. Chem. A* 2004, **108**, 1990.

[43] P. Caravan, M. T. Greenfield, X. Li, A. D. Sherry, *Inorg. Chem.* 2001, **40**, 6580.

[44] D. H. Powell, O. M. Ni Dhubhghaill, D. Pubanz, L. Helm, Y. S. Lebedev, W. Schlaepfer, A. E. Merbach, *J. Am. Chem. Soc.* 1996, **118**, 9333.

[45] D. Esteban-Gómez, A. de Blas, T. Rodriguez-Blas, L. Helm, C. Platas-Iglesias, *ChemPhysChem* 2012, **13**, 3640.

[46] L. Tei, M. Botta, C. Lovazzano, A. Barge, L. Milone, S. Aime, *Magn. Reson. Chem.* 2008, **46**, S86.

[47] C. S. Bonnet, F. Buron, F. Caille, C. M. Shade, B. Drahos, L. Pellegatti, J. Zhng, S. Villette, L. Helm, C. Pichon, F. Suzenet, S. Petoud, E. Toth, *Chem. Eur. J.* 2012, **18**, 1419.

[48] M. Mato-Iglesias, C. Platas-Iglesias, K. Djanashvili, J. A. Peters, E. Toth, E. Balogh, R. N. Muller, L. VanderElst, A. de Blas, T. Rodríguez-Blas, *Chem. Commun.* 2005, 4729.

[49] a) A. D'Aléo, A. Picot, P. L. Baldeck, C. Andraud, O. Maury, *Inorg. Chem.* 2008, **47**, 10269; b) M. Starck, P. Kadjane, E. Bois, B. Darbouret, A. Incamps, R. Ziessel, L. J. Charbonnière, *Chem. Eur. J.* 2011, **17**, 9164.

[50] S. Comby, R. Scopelitti, D. Imbert, L. J. Charbonnière, R.; Ziessel, J.-C. G. Bünzli, *Inorg. Chem.* 2006, **45**, 3158; Ziessel, J.-C. G. Bünzli, *Inorg. Chem.* 2006, **45**, 3158.

[51] a) G. Bozoklu, C. Gateau, D. Imbert, J. Pécaut, K. Robeyns, Y. Filinchuk, F. Memon, G. Muller, M. Mazzanti, *J. Am. Chem. Soc.* 2012, **134**, 8372; b) M. Elhabiri, R. Scopellitti, J.-C. G. Bünzli, C. Piguet, *J. Am. Chem. Soc.* 1998, **120**, 2347; c) T. Liu, A. Nonat, M. Beyler, M. Regueiro-Figueroa, K. Nchimi Nono, O. Jeannin, F. Camerel, F. Debaene, S. Cianférani-Sanglier, R. Tripier, C. Platas-Iglesias, L. J. Charbonnière, *Angew. Chem. Int. Ed.* 2014, **53**, 7259.

[52] a) L. Aboshyan-Sorgho, C. Besnard, P. Pattison, K. R. Kittilstved, A. Aebischer, J.-C. G. Bünzli, A. Hauser, C. Piguet, *Angew. Chem. Int. Ed.* 2011, **50**, 4108; *Angew. Chem.* 2011, **123**, 4194; b) A. Nonat, M. Regueiro-Figueroa, D. Esteban-Gomez, A. de Blas, T. Rodriguez-Blas, C. Platas-Iglesias, L.J. Charbonnière, *Chem. Eur. J.* 2012, **18**, 8163.

[53] J. Olmsted, *J. Phys. Chem.* 1979, **83**, 2581.

[54] N. Weibel, L. J. Charbonnière, M. Guardigli, A. Roda, R. Ziessel, *J. Am. Chem. Soc.* 2004, **126**, 4888.

[55] H. Ishida, S. Tobita, Y. Hasegawa, R. Katoh, N. Noaki, *Coord. Chem. Rev.* 2010, **254**, 2449.

[56] P. K. Glasoe, F. A. Long, *J. Phys. Chem.* 1960, **64**, 188.

[57] D. M. Corsi, C. Platas-Iglesias, H. van Bekkum, J. A. Peters, *Magn. Reson. Chem.* 2001, **39**, 723.

[58] A. D. Becke, *J. Chem. Phys.* 1993, **98**, 5648.

[59] C. Lee, W. Yang, R. G. Parr, *Phys. Rev. B* 1988, **37**, 785.

[60] Gaussian 09, Revision B.01, M. J. Frisch, G. W. Trucks, H. B. Schlegel, G. E. Scuseria, M. A. Robb, J. R. Cheeseman, G. Scalmani, V. Barone, B. Mennucci, G. A. Petersson, H. Nakatsuji, M. Caricato, X. Li, H. P. Hratchian, A. F. Izmaylov, J. Bloino, G. Zheng, J. L. Sonnenberg, M. Hada, M. Ehara, K. Toyota, R. Fukuda, J. Hasegawa, M. Ishida, T. Nakajima, Y. Honda, O. Kitao, H. Nakai, T. Vreven, J. A. Montgomery Jr., J. E. Peralta, F. Ogliaro, M. Bearpark, J. J. Heyd, E. Brothers, K. N. Kudin, V. N. Staroverov, R. Kobayashi, J. Normand, K. Raghavachari, A. Rendell, J. C. Burant, S. S. Iyengar, J. Tomasi, M. Cossi, N. Rega, N. J. Millam, M. Klene, J. E. Knox, J. B. Cross, V. Bakken, C. Adamo, J. Jaramillo, R. Gomperts, R. E. Stratmann, O. Yazyev, A. J. Austin, R. Cammi, C. Pomelli, J. W. Ochterski, R. L. Martin, K. Morokuma, V. G. Zakrzewski, G. A. Voth, P. Salvador, J. J. Dannenberg, S. Dapprich, A. D. Daniels, Ö Farkas, J. B. Foresman, J. V. Ortiz, J. Cioslowski, D. J. Fox, Gaussian, Inc., Wallingford CT, **2009**.

[61] M. Dolg, H. Stoll, A. Savin, H. Preuss, *Theor. Chim. Acta* 1989, **75**, 173.

[62] J. Tomasi, B. Mennucci, R. Cammi, *Chem. Rev.* 2005, **105**, 2999.

[63] a) C. Peng, P. Y. Ayala, H. B. Schlegel, M. J. Frisch, *J. Comput. Chem.* 1996, **17**, 49; b) C. Peng, H. B. Schlegel, *Isr. J. Chem.* 1994, **34**, 449.

[64] K. Fukui, *Acc. Chem. Res.* 1981, **14**, 363.

[65] R. Ditchfield, *Mol. Phys.* 1974, **27**, 789.

[66] M. Rezaei-Sameti, *J. Mol. Struct.* 2008, **867**, 122.